arXiv:1302.0579v3 [quant-ph] 5 Mar 2013

A Universal Quantum Circuit Scheme For Finding Complex Eigenvalues of Non-Unitary Matrices: Simulation of Resonance States

Anmer Daskin,[1] Ananth Grama,[1] and Sabre Kais[2, 3]

[1] *Department of Computer Science, Purdue University, West Lafayette, IN, 47907 USA*
[2] *Department of Chemistry, Department of Physics and Birck Nanotechnology Center, Purdue University, West Lafayette, IN 47907 USA*
[3] *Qatar Environment and Energy Research Institute, Doha, Qatar*

We present a general quantum circuit design for finding eigenvalues of non-unitary matrices on quantum computers using the iterative phase estimation algorithm. In particular, we show how the method can be used for the simulation of resonance states for quantum systems.

I. INTRODUCTION

In the circuit model of quantum computation, a controlled quantum system, considered to be a quantum computer, propagates from one state to another through the application of a local propagator called a quantum gate. A given algorithm, or computation, can be implemented on a quantum computer using a sequence of quantum gates. These gates can be represented by unitary matrices in the computational basis. While this unitary representation is adequate for many problems, it impedes application of quantum computing to new problems, where computational bases can only be described through non-unitary matrices. Furthermore, any attempt at approximation of these non-unitary parts negatively impacts the accuracy of the results. For instance, the algorithm of Harrow et. al [1] for solving linear systems of equations requires a non-unitary quantum gate. The circuit designed for this algorithm [2] uses an approximated gate for the non-unitary parts.

Quantum algorithms are known to be more efficient than their classical counterparts. One of these algorithms is the phase estimation algorithm [3–5], used for finding the eigenvalues of a given unitary matrix, or equivalently, the eigen-energies of the corresponding quantum system. The algorithm has been applied in quantum chemistry to obtain energies of molecular systems [6–10]. The algorithm has also been demonstrated experimentally[11, 12]. However, the simulation of non-hermitian matrices in quantum theory requires the simulation of non-unitary evolution matrices.

It has been shown that a quantum circuit can be generalized to a non-unitary circuit, whose constituents are non-unitary gates representing quantum measurement. Furthermore, it is shown that a specific type of one-qubit non-unitary gates, the controlled-NOT gate, and all one-qubit unitary gates constitute a universal set of gates for the non-unitary quantum circuit without the necessity of introducing ancilla qubits [13]. Recently, Nori et al. [14], proposed a measurement-based quantum algorithm for finding eigenvalues of non-unitary matrices. Their method draws on ideas from conventional phase estimation algorithm, frequent measurement, and techniques in one-qubit state tomography.

In this paper, we introduce a systematic way of estimating the complex eigenvalues of a general matrix using the iterative phase estimation algorithm with a programmable circuit design [15]. Our model can also be used as a general circuit equivalent for non-unitary matrices. We also present the application of our method to the example of non-hermitian Hamiltonians, which exhibit predissociating resonances. Since the circuit design is universal, it can be used to estimate the eigenvalues of any given system.

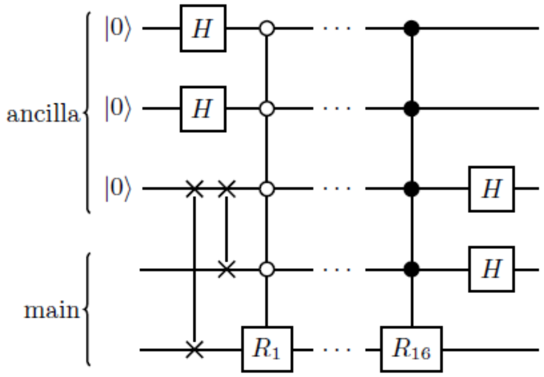

FIG. 1: Universal circuit design illustrated for two qubit operators: The uniformly controlled gates in the middle form all elements of U on the diagonal of V. The Hadamards at the end carry the same row elements to the first rows of each V_i. The initial Hadamards and the SWAPs modify the input.

II. UNIVERSAL CIRCUIT FOR NON-UNITARY MATRICES

Recently [15], we described a universal programmable circuit design that can be used to simulate any given matrix by simply determining the angle values for gates using matrix elements. This universal circuit, illustrated in Fig.1 for two qubit systems, is constructed as follows: For an arbitrary n-qubit system represented by an $N \times N$ matrix U (where $N = 2^n$), $(n+1)$ ancilla qubits are used to control $N \times N$ block quantum operations in order to generate circuit equivalences for rows of U independently.

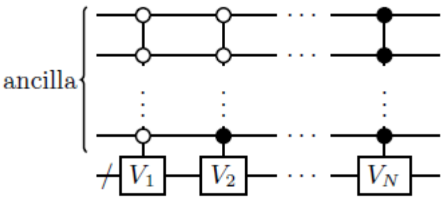

FIG. 2: Each block operations forms a different row of the given matrix as their leading row.

This is shown in Fig.2.

The matrix representation of Fig.2, V, has N block matrices located on its diagonal. Each of these blocks, V_i, generates the ith row of the given matrix as their first rows (the elements of V outside of the blocks are zero).

The relationship between an arbitrary input, $|\psi\rangle$, to the system U, and the corresponding output, $|\beta\rangle$, can be defined as $U|\psi\rangle = |\beta\rangle$. Using a modified input, $|\varphi\rangle$, the system with the ancilla, V, can also be used to simulate the application of U on predetermined N output states obtained from $V|\varphi\rangle$:

$$V|\varphi\rangle = \begin{pmatrix} V_1 & & & \\ & V_2 & & \\ & & \ddots & \\ & & & V_N \end{pmatrix} |\varphi\rangle = \begin{pmatrix} \kappa\beta_1 \\ \vdots \\ \kappa\beta_2 \\ \vdots \\ \kappa\beta_N \\ \vdots \end{pmatrix}, \tag{1}$$

in which the states: $\kappa\beta_1|0\dots000{-}0\dots0\rangle$, $\kappa\beta_1|0\dots010{-}0\dots0\rangle$, $\dots, \kappa\beta_N|1\dots110-0\dots0\rangle$, are exactly the same as the output we get from $U|\psi\rangle = |\beta\rangle$, with a normalization constant κ (the dashes are used to separate the ancilla and the *main* qubits). Next, the construction of V and $|\varphi\rangle$ in Eq.(1) are explained in following three steps: *Formation, Combination,* and *Input Modification.* These three steps result in the circuit shown in Fig.1.

1. *Formation step:*

Each element of U is formed using one rotation gate R_j located on the diagonal of V_f. V_f corresponds to a $2N^2 \times 2N^2$ matrix representing the *Formation* step:

$$V_f = \begin{pmatrix} R_1 & & \\ & \ddots & \\ & & R_{N^2} \end{pmatrix}, \; R_j(\theta_j) = \begin{pmatrix} cos(\frac{\theta_j}{2}) & sin(\frac{\theta_j}{2}) \\ -sin(\frac{\theta_j}{2}) & cos(\frac{\theta_j}{2}) \end{pmatrix}, \tag{2}$$

where R_j creates the jth-element, u_j, of U by the equality $cos(\frac{\theta_j}{2}) = u_j$. Here, we have used rotations around the y-axis. However, for the complex elements of U, a combination of R_z and R_y gates are needed for each R_j. The circuit equivalent of the matrix V_f constitutes N^2 uniformly controlled rotation gates (the total number of elements of U) operating on the last qubit ((2n+1)st qubit).

2. *Combination step:*

In this step, we bring the same row elements of U to the leading rows of each V_i by applying a combination matrix V_c to V_f, formed in the previous step: $V = V_cV_f$. This is described as:

$$\begin{pmatrix} V_c^{(1)} & & & \\ & V_c^{(2)} & & \\ & & \ddots & \\ & & & V_c^{(N)} \end{pmatrix} \begin{pmatrix} u_{11} & \sqrt{1-u_{11}} & & & \\ -\sqrt{1-u_{11}} & u_{11} & & & \\ & & \ddots & & \\ & & & u_{NN} & \sqrt{1-u_{NN}} \\ & & & -\sqrt{1-u_{NN}} & u_{NN} \end{pmatrix} = \begin{pmatrix} ku_{11} & * & ku_{12} & \dots & * & ku_{1N} & & & & & & \\ \vdots & \vdots & \vdots & & \vdots & \vdots & & & & & & \\ & & & & & & \ddots & & & & & \\ & & & & & & ku_{N1} & * & ku_{N2} & \dots & * & ku_{NN} \\ & & & & & & \vdots & \vdots & \vdots & & \vdots & \vdots \end{pmatrix}, \tag{3}$$

where each $V_c^{(i)}$ has the following form:

$$V_c^{(i)} = \begin{pmatrix} k & 0 & \dots & k & 0 \\ 0 & k & \dots & 0 & k \\ \vdots & \vdots & \vdots & \vdots & \vdots \\ k & 0 & \dots & k & 0 \\ 0 & k & \dots & 0 & k \end{pmatrix}_{2N\times 2N}. \tag{4}$$

For a system of $(n+1)$ qubits, the matrix in Eq.(4) represents the Hadamard gates on the first n qubits with $k = 1/\sqrt{2^n}$. Thus, for a system of $2n+1$ qubits, V_c can be defined as the application of the Hadamard gates to $(n+1)$th, nth, ..., 3rd, and 2nd qubits from the bottom in the circuit.

3. *Input modification step:*

After forming all the rows of U through the leading rows of each block V_i, we transform the input so that the resulting output includes the simulation results defined in Eq.(1). The initial input to the final matrix V in Eq.3 can be defined as $|\tilde{\psi}\rangle = |0..0\rangle \otimes |\psi\rangle$ where $|0...0\rangle$ is the input to the ancilla qubits. In the application of V, we also

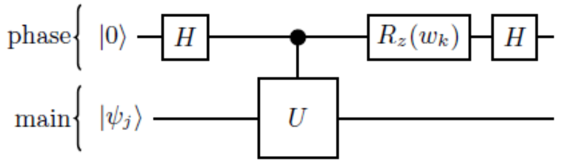

FIG. 3: The iterative phase estimation algorithm for the kth iteration [3–5]. In the circuit $|\psi_j\rangle$ is an eigenvalue of U, and the angle w_k of the R_z gate depends on the previously measured bits defined as $w_k = -2\pi(0.0x_kx_{k-1}...x_m)_{binary}$, where m is the number of digits determining the accuracy of the phase ϕ_j. Note that w_k is zero in the first iteration of the algorithm.

need to disregard the effects of the elements represented by "$*$" between ku_{ij} and $ku_{i(j+1)}$. If the corresponding elements in the input $|\tilde{\psi}\rangle$ are made zero, as in Eq. (5), these elements are not-effective in the application of V to the following input state:

$$\begin{aligned}|\tilde{\psi}\rangle =&[\alpha_1\ \alpha_2\ \ldots\alpha_N\ 0\ldots0]^T \rightarrow\\ &[\kappa\alpha_1\ 0\ \kappa\alpha_2\ldots0\ \kappa\alpha_N\ldots\ \kappa\alpha_1\ 0\ \kappa\alpha_2\ \ldots\ 0\ \kappa\alpha_N]^T,\end{aligned} \tag{5}$$

where κ is a normalization constant. This modification can be achieved by applying Hadamard gates on the first n qubits, and sequential swap operations between the $(n+1)$th and the remaining last n qubits.

Consequently, the combination of these three steps yields the final circuit, which is shown in Fig.1 for a two qubit system. This circuit can be used to simulate any matrix U having matrix elements less than or equal to 1. Finally, the following normalized set of N states exactly simulates the given unitary U: $|0\ldots000-0\ldots0\rangle,\ldots|1\ldots110-0\ldots0\rangle$. For simplicity, in the phase estimation algorithm, we will swap the first n ancilla qubits with the main qubits and use the following states instead:

$$\begin{aligned}&|0\ldots0-0\ldots00\rangle\\&|0\ldots0-0\ldots01\rangle\\&\vdots\\&|0\ldots0-0\ldots10\rangle\\&|0\ldots0-1\ldots11\rangle\end{aligned} \tag{6}$$

III. FINDING EIGENVALUES OF NON-UNITARY MATRICES

The polar form of a complex eigenvalue, λ_j, belonging to a matrix, U, can be written as:

$$\lambda_j = r_j\ e^{-i2\pi\phi_j}, \tag{7}$$

where ϕ_j is the phase and $r_j = |\lambda_j|$ is the magnitude of the jth eigenvalue. For unitary matrices, since $|\lambda_j|$ is equal to 1, the phase estimation algorithm (PEA) is a well-known efficient quantum algorithm used to estimate the phase, ϕ_j, and consequently, the corresponding eigenvalue, λ_j. The iterative phase estimation algorithm IPEA [3–5] shown in Fig.6 can also be used to estimate the value of the phase, ϕ_j. In each iteration of the phase estimation process, we estimate one bit of the m-digit binary expansion of the phase represented as:

$$\begin{aligned}\phi_j =&(0.x_1x_2...x_m)_{binary}\\ =&x_12^{-1}+x_22^{-2}...\ x_{m-1}2^{-m+1}+x_m2^{-m},\end{aligned} \tag{8}$$

where m is the total number of iterations, which determines the precision. x_k is the binary value found from the kth iteration of the IPEA using the 2^{m-k}th power of the matrix, $U^{2^{m-k}}$.

However, for non-unitary matrices, the phase estimation algorithm alone is not enough. This is because two parameters, ϕ_j and r_j, must be found to compute the eigenvalue. In the following sections, we show that by applying the iterative version of the phase estimation algorithm to the general circuit described in the previous section, parameters ϕ_j and r_j can be determined, and hence eigenvalues of non-unitary matrices can also be found by the phase estimation algorithm without additional cost. Since our circuit design has a fixed size and scheme, the application of IPEA to the circuit design also has a fixed design. Therefore, we only need to set the angle values in each iteration of IPEA.

A. Estimation of ϕ_j

To use the general circuit design shown in Fig.1 for 4×4 matrices, within the IPEA framework, we need to determine the relationship between the chosen states and the phase qubit resulting in the measurement. As described in the previous section, the circuit scales the expected output of the chosen states by κ, which clearly originates from the Hadamard gates. In phase estimation, since all of the gates are controlled by the upper qubit, this scaling effect of κ exists only when the phase qubit is one. In order to have the same scaling when the phase qubit is zero, we allow the Hadamard gates in the circuit to operate without any control qubit. Therefore, controlling the swap gates at the beginning and at the end of the circuit do not affect the chosen states. Hence, they are also allowed to operate without the control on the phase qubit. The resulting circuit is shown for two qubit systems in Fig.4. Here, we control all operations except the Hadamard and the swap gates by the phase qubit.

We estimate the phase on the selected N states, where the ancilla is zero in the output. In one iteration of the phase estimation algorithm, the effect of the eigenvalue, represented in polar form, can be observed in the evolution of the system as follows: After the first Hadamard gate on the phase qubit, as seen in the circuit in Fig.(6), and the controlled operation (as stated above, the Hadamard and the swap gates are not controlled), we have the following wave function describing the chosen states in the first iteration (the ancilla is ignored since it is zero in the chosen states):

$$\Psi_1 = \frac{\kappa}{\sqrt{2}}(|0\rangle|\psi_j\rangle + e^{i2\pi(0.x_1)}|\lambda_j||1\rangle|\psi_j\rangle), \tag{9}$$

where $|\psi_j\rangle$ is the input, an estimate of the eigenvector, and the first qubit is the phase qubit. Application of the rotation gate around the z-axis on the phase qubit in the circuit guarantees that only one bit, x_k in $0.x_k$, of the phase is estimated in each iteration. After the last Hadamard applied to the phase qubit, the state in Eq.(9) becomes:

$$\Psi_2 = \frac{\kappa}{\sqrt{2}}((\frac{|0\rangle + |1\rangle}{\sqrt{2}})|\psi_j\rangle + e^{i2\pi(0.x_1)}|\lambda_j|(\frac{|0\rangle - |1\rangle}{\sqrt{2}})|\psi_j\rangle) \tag{10}$$

or more concisely:

$$\Psi_2 = \frac{\kappa}{2}((1+e^{i2\pi(0.x_1)}|\lambda_j|)|0\rangle + (1-e^{i2\pi(0.x_1)}|\lambda_j|)|1\rangle)|\psi_j\rangle. \tag{11}$$

When $x_1 = 0$, since $e^{i2\pi 0} = 1$, the above equation reduces to:

$$\Psi_2 = \frac{\kappa}{2}((1 + |\lambda_j|)|0\rangle + (1 - |\lambda_j|)|1\rangle)|\psi_j\rangle. \tag{12}$$

In the case when $x_1 = 1$, Eq.(11) becomes:

$$\Psi_2 = \frac{\kappa}{2}((1 - |\lambda_j|)|0\rangle + (1 + |\lambda_j|)|1\rangle)|\psi_j\rangle. \tag{13}$$

Since $\frac{\kappa}{2}(1 - |\lambda_j|) \leq \frac{\kappa}{2}(1 + |\lambda_j|)$; if the phase bit is 0, then $x_1 = 0$. If the phase bit is 1, then the $x_1 = 1$. Thus, the measurement on the phase qubit determines x_1. In each iteration of the phase estimation algorithm, a different bit of the phase is determined in this manner. For the kth iteration of the phase estimation algorithm to determine the kth digit of the phase, we see $\frac{\kappa}{2}(1 - |\lambda_j|^{2^k}) \leq \frac{\kappa}{2}(1 + |\lambda_j|^{2^k})$. Hence, for $|\lambda_j| < 1$, the more we increase the power of U or the accuracy, the more the amplitudes of the states, $|0\rangle$ and $|1\rangle$, come closer.

B. Computing $|\lambda_j|$

As we have shown above, the output probability of the phase qubit when the ancilla is zero is determined by $\frac{\kappa}{2}((1 + |\lambda_j|)$. We measure $|0\rangle$ or $|1\rangle$ with probability P equal to $\frac{\kappa}{2}((1 + |\lambda_j|)$. Hence, we get

$$\begin{aligned} P &= (\frac{\kappa}{2}((1 + |\lambda_j|))^2, \\ |\lambda_j| &= \frac{2\sqrt{P}}{\kappa} - 1. \end{aligned} \tag{14}$$

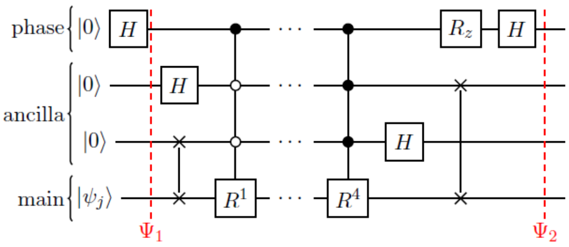

FIG. 4: The iterative phase estimation algorithm with the circuit shown for a 2×2 matrix. The decomposition of the middle multi control network requires 16 CNOTs and 16 single rotation gates.

Since κ and P are known (for a 2×2 matrix, the value of κ is 2 due to two Hadamard gates in the circuit), $|\lambda_j|$ can be determined from Eq.(14). Therefore, the accuracy of the estimate value of $|\lambda_j|$ can be further improved by using all iterations of the phase estimation algorithm: For the kth iteration, as a general form, the following is obtained:

$$\begin{aligned} P_{(k)} &= (\frac{\kappa}{2}((1 + |\lambda_j|^{2^k}))^2, \\ |\lambda_j|^{2^k} &= \frac{2\sqrt{P_{(k)}}}{\kappa} - 1. \end{aligned} \tag{15}$$

Taking the average of the estimates from different phase estimation iterations, the estimate of $|\lambda_j|$ may become more accurate. Finally, by using values of $|\lambda_j|$ and ϕ_j in Eq. (7), we can compute the eigenvalue of the non-unitary matrix.

Note that the complexity of computing the power of matrix U on classical computers is $O(mM)$, where m is the number of iterations and M is the complexity of matrix multiplication (this is estimated using the successive squaring method).

IV. APPLICATION TO NON-HERMITIAN QUANTUM SYSTEMS

Suppose we have the non-unitary operator $U = e^{-i\mathcal{H}t/\hbar}$ for a non-hermitian Hamiltonian $\mathcal{H}$ with energy eigenstates $|\psi_j\rangle$ and corresponding energy eigenvalues E_j, i.e., $\mathcal{H}|\psi_j\rangle = E_j|\psi_j\rangle$. Since E_j is an eigenvalue of $\mathcal{H}$; if t and $\hbar$ are set to 1, then e^{-iE_j} is the eigenvalue of U. Therefore, a $N \times N$ non-unitary transformation U has eigenvectors $|\varphi_1\rangle$, $|\varphi_2\rangle$, ..., $|\varphi_N\rangle$, with corresponding eigenvalues $\lambda_j = |\lambda_j|e^{-i2\pi\phi_j}$. As shown in Sec.III, the eigenvalue λ_j of the matrix U can be estimated. This also allows us to determine the corresponding eigenvalue E_j of the Hamiltonian $\mathcal{H}$ from $\lambda_j = e^{-iE_j}$.

A. Example: Simulation of Resonance States

As an example, we consider the following radial Hamiltonian:

$$\mathcal{H} = -\frac{1}{2}\frac{d}{dr}(r^2\frac{d}{dr}) + (\frac{r^2}{2} - J)e^{-ar^2}, \tag{16}$$

where a and J are free parameters. The potential in the above Hamiltonian exhibits predissociating resonances [16], shown in Fig.5. Because of the resonances, the matrix for this Hamiltonian is non-hermitian, and so the time evolution operator found from $U = e^{-i\mathcal{H}t/\hbar}$ is non-unitary. We will use our method described above to simulate this non-unitary operator and determine the complex eigenvalues of $\mathcal{H}$. As a basis function for computing the matrix elements of the Hamiltonian, we use the orthonormalized eigenfunctions of the harmonic oscillator, where mass equals one and the frequency equals a ref.[16]:

$$\Psi_n(a:r) = (\frac{a}{\pi})^{1/4}\frac{1}{\sqrt{2^n n!}}e^{-(ar^2/2)}H_n(\sqrt{a}r). \tag{17}$$

H_n are the Hermite polynomials of order n. For illustration purposes, we use only two bases with $n = 0$ and $n = 1$ to determine the elements of the 2×2 Hamiltonian matrix. The matrix is found as [17]:

$$H = \begin{pmatrix} 1.4216 - 0.1576i & 0.2782 + 0.2802i \\ 0.2782 + 0.2802i & 0.6807 - 0.2361i \end{pmatrix}, \tag{18}$$

which has the eigenvector:

$$|\psi_j\rangle = \begin{pmatrix} -0.3790 - 0.1962i \\ 0.9044 \end{pmatrix}, \tag{19}$$

and the ground state eigenenergy $(0.6249 - 0.4139i)$. The time evolution operator for this Hamiltonian is

$$\begin{aligned} U &= e^{i\mathcal{H}} \\ &= \begin{pmatrix} 0.2588 + 1.1214i & -0.4569 - 0.1109i \\ -0.4569 - 0.1109i & 1.0594 + 0.7394i \end{pmatrix}, \end{aligned} \tag{20}$$

with eigenvalue $1.2268 + 0.8849i$. From the simulation output, as shown in Fig.6, we find the eigenvalue of U as $1.2259 + 0.8861i$, and so the eigenvalue of $\mathcal{H}$ as $0.6259 - 0.4139i$, which gives an error in the order of 10^{-3}. This comes from computer round-off and the limited available powers of U (when the power of lambda goes to zero, we can no longer distinguish between $|0\rangle$ and $|1\rangle$ on the phase qubit; the probabilities becomes the same). The simulation details and the decomposition of the circuit are shown in the Appendix A.

V. CONCLUSION

We have presented a general scheme for the execution of the phase estimation algorithm for non-unitary matrices. Since the circuit design used for non-unitary matrices is a general programmable circuit, the circuit for the phase estimation algorithm is also universal: It can be used for any type of matrix to compute its eigenvalues. We have shown that the complex eigenvalues of non-hermitian quantum systems can be found by using this method. As an example we have shown how to obtain resonances for a model Hamiltonian used to describe predissociating resonances. The method is general, and can be used to simulate resonances of atomic and molecular systems.

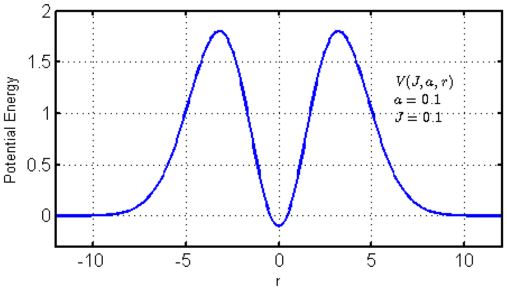

FIG. 5: The potential energy, $V(J, a, r)$, as a function of the radial distance, r. The values of a and J are set to 0.1.

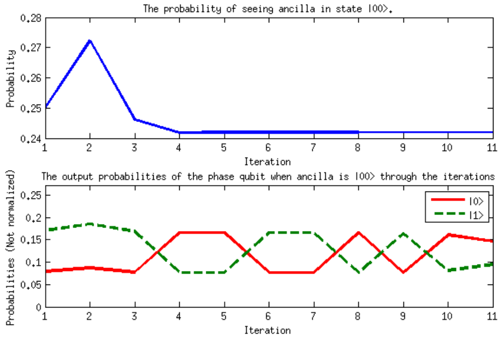

FIG. 6: Output of the iterative phase estimation algorithm.

VI. ACKNOWLEDGEMENT

We thank Pablo Serra for providing the Hamiltonian matrix used as an example in this paper. This work is supported by the NSF Centers for Chemical Innovation: Quantum Information for Quantum Chemistry, CHE-1037992.

Appendix A: Simulation Details

1. The decomposition of a multi controlled network

The uniformly controlled networks such as the one in Fig.7a controlled by k qubits can be decomposed in terms of 2^k CNOT gates and 2^k single rotation gates[18]. For instance, the circuit as illustrated for $k = 2$ in Fig.7a can be decomposed as in Fig.7b. The angle values in the decomposed circuit are solutions of the system of the

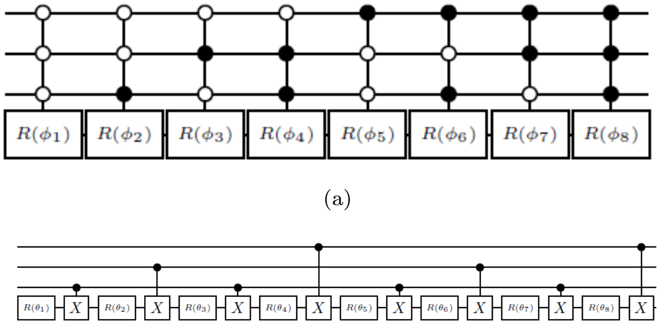

(a)

(b)

FIG. 7: (a) A uniformly controlled multi-qubit network. (b) The decomposition of the network in (a) into CNOT and single quantum gates. The change of the bits in the gray code representations determines the control qubit for the CNOT gates. The network in the phase estimation algorithm includes two consecutive circuits such as in (b) with R_z and R_y single gates.

linear equation $M^k\boldsymbol{\theta} = \boldsymbol{\phi}$:

$$M^k \begin{pmatrix} \theta_1 \\ \theta_2 \\ \vdots \\ \theta_{2^k} \end{pmatrix} = \begin{pmatrix} \phi_1 \\ \phi_2 \\ \vdots \\ \phi_{2^k} \end{pmatrix}, \tag{A1}$$

where k is the number of control qubits in the network, and the entries of M are defined as:

$$M_{ij} = (-1)^{b_{i-1} \cdot g_{j-1}}, \tag{A2}$$

in which the power term is found by taking the dot product of the standard binary code of the index $i-1$, b_{i-1}, and the binary representation of $j-1$th Gray coded integer, g_{j-1}. Since M^k is a column permuted version of the Hadamard matrix, we see that M is unitary. Thus, $(M^k)^{-1} = 2^{-k}(M^k)^T$, and the new angle values in the decomposed circuit are results of the matrix vector multiplication[18]:

$$\boldsymbol{\theta} = 2^{-k}(M^k)^T\boldsymbol{\phi}. \tag{A3}$$

2. The Decomposition of Multi-controlled network part in Fig.4

In Fig.4, we have a multi controlled network composed of 4 gates. This network basically comes from the *Formation* step of the circuit design method, which has been represented in matrix form as V_f in Eq.(2). Since the elements of U are complex, we need to have rotations around the $z-$axis and the $y-$axis. Hence, the above matrix is the product of two matrices V_f^z for rotation around the z-axis, and V_f^y for rotations around the y-axis: $V_f = V_f^z V_f^y$:

$$V_f = \begin{pmatrix} R_1^z & & \\ & \ddots & \\ & & R_{N^2}^z \end{pmatrix} \begin{pmatrix} R_1^y & & \\ & \ddots & \\ & & R_{N^2}^y \end{pmatrix} \tag{A4}$$

To complete this network to a whole uniformly controlled network, we assume that the initial four other gates are identity. Hence, the final decomposition for 2×2 matrix, the decomposed circuit includes: 4 Hadamard gates, 16 CNOT and 16 single gates (8 CNOTs and 8 Ry gates for the V_f^y; and 8 CNOTs and 8 Ry gates for the V_f^z), and 2 swaps. The probability changes for the chosen state and the phase qubit in the simulation for this decomposed circuit are shown in Fig.6.

BIBLIOGRAPHY

[1] A. W. Harrow, A. Hassidim, and S. Lloyd, Phys. Rev. Lett. **103**, 150502 (2009)
[2] Y. Cao, A. Daskin, S. Frankel, and S. Kais, Molecular Physics **110**, 1675 (2012)
[3] M. Dobšíček, G. Johansson, V. Shumeiko, and G. Wendin, Phys. Rev. A **76**, 030306 (Sep 2007)
[4] D. S. Abrams and S. Lloyd, Phys. Rev. Lett. **83**, 5162 (Dec 1999)
[5] A. Kitaev, Electronic Colloquium on Computational Complexity (ECCC) **3** (1996)
[6] A. Aspuru-Guzik, A. Dutoi, P. Love, and M. Head-Gordon, Science **309**, 1704 (2005)
[7] H. Wang, S. Kais, A. Aspuru-Guzik, and M. Hoffmann, Phys.Chem.Chem.Phys. **10**, 5388 (2008)
[8] D. Lidar and H. Wang, Phys. Rev. E **59**, 2429 (1999)
[9] L. Veis and J. Pittner, J. Chem. Phys. **133**, 194106 (2010)
[10] A. Daskin and S. Kais, J. Chem. Phys. **134**, 144112 (2011)
[11] B. P. Lanyon, J. D. Whitfield, G. G. Gillett, M. E. Goggin, M. P. Almeida, I. Kassal, J. D. Biamonte, M. Mohseni, B. J. Powell, M. Barbieri, A. Aspuru-Guzik, and A. G. White, Nature Chemistry **2**, 106 (2010), ISSN 1755-4330
[12] D. Lu, B. Xu, N. Xu, Z. Li, H. Chen, X. Peng, R. Xu, and J. Du, Phys. Chem. Chem. Phys. **14**, 9411 (2012)
[13] H. Terashima and M. Ueda, International Journal of Quantum Information **03**, 633 (2005)
[14] H. Wang, L. Wu, Y. Liu, and F. Nori, Phys. Rev. A **82**, 062303 (Dec 2010)
[15] A. Daskin, A. Grama, G. Kollias, and S. Kais, The Journal of Chemical Physics **137**, 234112 (2012)
[16] P. Serra, S. Kais, and N. Moiseyev, Phys. Rev. A **64**, 062502 (Nov 2001)
[17] This matrix is given by Pablo Serra, private communication, 2012. [16]
[18] M. Möttönen, J. J. Vartiainen, V. Bergholm, and M. M. Salomaa, Phys. Rev. Lett. **93**, 130502 (2004)